Life Sciences 230 (2019) 97–103

Contents lists available at ScienceDirect

Life Sciences

journal homepage: www.elsevier.com/locate/lifescie

Honokiol alleviates acetaminophen-induced hepatotoxicity *via* decreasing generation of acetaminophen-protein adducts in liver

Feng-Ling Yu[a], Jun-Wen Wu[b,*], He Zhu[c,d,**]

[a] Linyi Central Hospital, Linyi 276400, China
[b] Jiangsu Hengrui Medicine Co., Ltd., Nanjing 210000, China
[c] Department of Pharmaceutical Analysis and Metabolomics, Jiangsu Province Academy of Traditional Chinese Medicine and Jiangsu Branch of China Academy of Chinese Medical Sciences, Nanjing 210028, China
[d] Linyi Lab Pharmaceutical Technology Co., Ltd., Linyi 276017, China

ARTICLE INFO

Keywords:
Acetaminophen
Honokiol
Acetaminophen-protein adducts
CYP2E1
Glutathione
NRF2

ABSTRACT

Aim: Acetaminophen (APAP) overdose is the most frequent cause of drug-induced liver damage. *Magnolia officinalis* is a traditional hepatoprotective Chinese medicine and Honokiol (HO) is the major active constituent. The present study was to investigate the effect of HO on APAP-induced hepatotoxicity and related mechanisms.
Main methods: Four groups of mice were subjected to treatment as vehicle, APAP, APAP + HO and APAP + HO + NRF2 inhibitor. The morphological and biochemical assessments were used to evaluate the hepatoprotective effects. The extent of APAP-protein adducts was determined through evaluate the hepatic content 3-(cystein-S-yl)acetaminophen (APAP-Cys), the hydrolysis products of APAP-protein adducts. The activities of CYP2E1, CYP1A2 and CYP3A4 were evaluated by cocktail incubation, and the protein expression levels of NRF2, GCLC, GCLM, GS and GST were evaluated by western blot analysis.
Key findings: Morphological and biochemical assessments clearly demonstrated that HO could alleviate APAP-induced liver damage. The hepatoprotective effect of HO was positively associated with the reduction of APAP-protein adducts. Further investigation suggested that HO induced inhibition of CYP 2E1 and CYP2A1 as well as upregulation of GSH co-contributed to the reduction of APAP-protein adducts. Furthermore, HO induced activations of NRF2 and its target enzymes, such as GCLC, GCLM and GST, gave rise to the upregulation of GSH.
Significance: Our results suggested that HO could alleviate APAP-induced liver damage through reducing the generation of APAP-protein adducts, which might be mediated by inhibiting the activity of CYP 2E1 and CYP2A1 as well as enhancing the generation of GSH *via* NRF2 pathway.

1. Introduction

Acetaminophen (APAP, also named as paracetamol) is a worldwide used analgesic and antipyretic drug [1]. Although relatively safe at therapeutic doses, APAP in high doses can cause severe liver damage. Typically, in the United States and the United Kingdom, APAP overdose is associated with the leading cause of drug-induced hepatotoxicity and acute liver failure [2,3]. CYP450-dependent biotransformation of APAP to its reactive metabolite has been clearly identified as the mechanism mediating APAP-induced liver damage. In the therapeutic dose condition, APAP is converted to *N*-acetyl-p-benzoquinone imine (NAPQI) by CYP 2E1, CYP1A2 and CYP3A4 [4,5]. Subsequently, NAPQI is detoxified by glutathione (GSH), a tripeptide that detoxifying electrophiles and relieving oxidative stress, with the aid of glutathione S-transferase (GST). However, in the overdose condition, excess NAPQI rapidly depletes hepatic GSH, whereas, the remaining NAPQI covalently binds to sulfhydryl groups on cysteine residues of hepatocellular proteins, generates APAP-protein adducts and finally triggers mitochondrial

Abbreviations: ALT, alanine aminotransferase; APAP, acetaminophen; APAP-Cys, 3-(cystein-S-yl)acetaminophen; AST, aspartate aminotransferase; CMT, clomethiazole; FDA, US Food and Drug Administration; GCLC, glutamate-cysteine ligase catalytic subunit; GCLM, glutamate-cysteine ligase regulatory subunit; GS, glutathione synthetase; GSH, glutathione; GST, glutathione S-transferase; H&E, hematoxylin-eosin; HO, honokiol; i.g., intragastric; i.p., intraperitoneal; KET, ketoconazol; NAPQI, *N*-acetyl-p-benzoquinone imine; NPF, α-naphthoflavone; NRF2, nuclear factor (erythroid-derived 2)-like 2; S.D., standard deviation

* Corresponding author.
** Correspondence to: H. Zhu, Jiangsu Province Academy of Traditional Chinese Medicine and Jiangsu Branch of China Academy of Chinese Medical Sciences, Nanjing 210028, China.
E-mail addresses: wuxiaobaivip@163.com (J.-W. Wu), zhuhev@163.com (H. Zhu).

https://doi.org/10.1016/j.lfs.2019.05.062
Received 13 April 2019; Received in revised form 22 May 2019; Accepted 23 May 2019
Available online 24 May 2019

dysfunction and necrosis [6,7]. The extent of APAP-protein adducts in the liver is positively related with the liver damage. Many methods have been developed to evaluate the contents of APAP-protein adducts [8–10]. Determination of 3-(cystein-S-yl)acetaminophen (APAP-Cys), the hydrolysis products of APAP-protein adducts, is one of the most convenient methods to evaluate the contents of APAP-protein adducts [11–13].

Magnolia officinalis (Magnoliaceae) is mainly found in East Asia, and its bark has been widely utilized in China to treat liver disease [14]. Honokiol (HO) is one of its bioactive components and exhibits strong antioxidant, anti-inflammatory and anti-tumor effects [15]. Recent studies showed that HO benefits lipopolysaccharide-induced liver damage through inhibiting cytokine production and oxidative stress [16], ameliorates alcoholic steatosis *via* blocking fatty acid synthesis [14], attenuates non-alcoholic steatohepatitis by polarizing macrophages to M2 phenotype [17] and improving hepatic steatosis [18], and relieves oxidative damage in hepatocytes by activating Sirtuin3 [19]. Base on those observations, we proposed a hypothesis that HO could show protective effects against APAP-induced liver damage.

In this study, the protective effects of HO against APAP-induced hepatotoxicity and the potential mechanisms involved were investigated, which could verify our hypothesis and improve better understanding the hepatoprotective effects of HO.

2. Material and methods

2.1. Materials and reagents

APAP, diazepam, phenacetin, chlorzoxazone, donepezil and ketoconazole (KET) were purchased from National Institutes for Food and Drug Control (Beijing, China). Testosterone and 6β-hydroxy-testosterone were obtained from Shanghai J&K Scientific LTD (Shanghai, China), 6-hydroxy-chlorzoxazone was supplied by Toronto Research Chemicals Inc. (Toronto, Canada), clomethiazole (CMT) was obtained from Sigma-Aldrich Chemical Co. (St. Louis, USA) and α-naphthoflavone (NPF) was supplied from Acros Organics (New Jersey, USA). APAP used in the animal study was obtained from Linyi Central Hospital, Linyi, China. HPLC grade methanol was purchased from Merck Company (Darmstadt, Germany). All other reagents were of analytical grade and obtained from commercial sources.

2.2. Synthesis of APAP-Cys

APAP-Cys (Fig. 1) was custom-synthesized in the laboratory following the procedures described in the literature [13,20,21]. The purity of the compound was shown by HPLC to be > 95%. The chemical structure of the synthesized APAP-Cys was further confirmed by mass spectroscopy analysis (Supplementary Fig. 1). These mass data are in agreement with previously published data of synthesized APAP-Cys [13,20,21].

2.3. Animals and dosing

Male Balb/c mice (20–22 g) were supplied by Shanghai Slac Laboratory Animal Co., Ltd., China. All animals were housed under controlled temperature 25 ± 1 °C, relative humidity 40–70%. The animal care and use were in accordance with the Regulations of Experimental Animal Administration issued by the Ministry of Science and Technology of China, and the experimental protocols were approved by the Animal Affairs Committee of Jiangsu Province Academy of Traditional Chinese Medicine. All animals were fasted overnight before experiment.

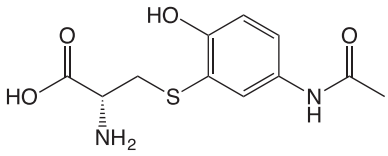

Fig. 1. Chemical structure of APAP-Cys.

Twenty-four mice were randomly divided into four groups, which were vehicle, APAP, APAP plus HO and NRF2 inhibitor groups. The preparation of HO for intragastric (i.g.) administration was made by suspending it in 1% [w/v] sodium carboxymethyl cellulose (CMC-Na) and APAP for intraperitoneal (i.p.) was made by dissolving in normal saline. The vehicle group was i.g. 0.2 mL 1% CMC-Na solution and i.p. 0.1 mL normal saline, the APAP group was i.g. 0.2 mL 1% CMC-Na solution and i.p. APAP normal saline solution (200 mg/kg), the APAP plus HO group was i.g. HO suspension (100 mg/kg) and i.p. APAP normal saline solution (200 mg/kg), and the NRF2 inhibitor group was i.g. HO suspension (100 mg/kg) and i.p. APAP normal saline solution (200 mg/kg) 1 h after i.p. Brusatol (2 mg/kg). All animals were treated once per day at 9:00 a.m. for 7 consecutive days. One hour after the last dosing, each animal was sacrificed under anaesthetic, and liver was surgically excised and placed in liquid nitrogen or fixed in formaldehyde solution until needed, while serum was prepared and analyzed immediately.

2.4. Biochemical and histological assessments

Levels of alanine aminotransferase (ALT) and aspartate aminotransferase (AST) in serum and reduced GSH in liver tissues were measured using an assay kit (Nanjing Jiancheng Corp., Nanjing, China) according to the manufacturer's recommendations. Fixed hepatic tissues were embedded in paraffin, cut into 5 μm sections, stained with hematoxylin-eosin (H&E), and observed using a light microscope (200 ×).

2.5. Protein derived APAP-Cys preparation

Protein derived APAP-Cys was prepared according to published papers with slight optimizations [13,20,21]. Briefly, mouse liver (100 mg) was homogenized in 1 mL sodium acetate (10 mM, pH 6.5), sonicated for 10 s, centrifuged at 16,000*g* for 10 min, and the resulting supernatants were dialyzed (30 kDa molecular mass cut-off) against 4 L of 10 mM sodium acetate buffer. The dialysis buffer was replaced at 9 and 21 h and the dialyzed samples were concentrated to 1 mL after dialyzing 30 h. Concentrated samples (100 μL) were digested overnight with proteases and precipitated using cold methanol after adding diazepam (IS1, 1 μg/mL, 5 μL). The supernatants were evaporated at 40 °C under a steady nitrogen stream. The protein derived APAP-Cys containing residues were re-suspended by 120 μL mobile phase for analysis.

2.6. CYP450 metabolic enzyme activity assay

The mouse liver microsomes were prepared according to our published paper [22], and the effect of HO on the activities of CYP2E1, CYP1A2 and CYP3A4 were evaluated by cocktail incubation, as follow. The incubation mixtures containing pooled mice liver microsomes (final concentration 0.25 mg/mL), CYP2E1, CYP1A2 or CYP3A4 probe substrate (chlorzoxazone, phenacetin or testosterone, final concentration 50 μM) or blank control, HO or positive controls (CMT for CYP2E1, NPF for CYP1A2 and KET for CYP 3A4) were preincubated for 10 min at 37 °C, and the reaction initiated by the addition of NADPH (final concentration 2 μM). Each mixture was incubated for 20 min at 37 °C in a shaking water bath and the reaction terminated by adding 3-fold APAP (IS2, 5 μM) or donepezil (IS3, 10 μM) acetonitrile solution. The final concentrations of HO and positive controls in the incubation mixtures were 0.01, 0.1, 0.3, 1, 3, 10, 30 and 100 μM, and all the experiments were performed in sextuplicate. The concentrations of probe substrate metabolite (6-hydroxy-chlorzoxazone, APAP and 6β-hydroxy-testosterone) were calculated from the standard curves. The IC50

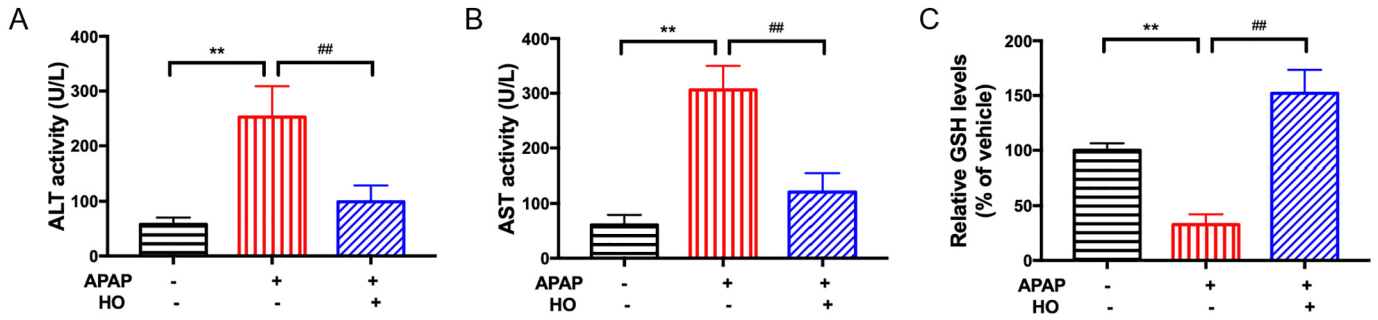

Fig. 2. Biochemical parameters in serum and GSH content in liver. (A) ALT, (B) AST and (C) GSH. Data are represented as the mean ± S.D. of six independent experiments. $^{**}p < 0.01$ *vs.* vehicle group, and $\#\#p < 0.01$ *vs.* APAP-treated group.

values were determined based on the concentration-inhibition curves.

2.7. Western blot analysis

Liver tissue homogenates were prepared with RIPA Buffer. Equal amount of denatured total protein (50 μg) was separated by 10% sodium dodecyl sulfate polyacrylamide gel electrophoresis and transferred onto a polyvinylidene difluoride membrane. The membrane was blocked by 5% fetal bovine serum and incubated with appropriate dilutions of primary antibody against nuclear factor (erythroid-derived 2)-like 2 (NRF2), glutamate-cysteine ligase regulatory subunit (GCLM), glutamate-cysteine ligase catalytic subunit (GCLC), glutathione synthetase (GS) or GST, respectively, followed by incubation with rabbit anti-mouse or goat anti-mouse HRP-conjugated secondary antibody. The intended protein was detected using ECL kit and normalized to the corresponding β-actin expression.

2.8. LC-MS/MS method validation

Determinations of APAP-Cys and 6-hydroxy-chlorzoxazone were carried out on an Agilent 1200 HPLC-6410B triple quadrupole mass spectrometer (Agilent Technologies, Palo Alto, USA). Chromatographic separations were performed on an Agilent Zorbmax SB-C18 column (2.1 mm × 15 cm, 5 μm, Agilent Technologies, Palo Alto, USA) with a security Guard-C18 (4 mm × 2.0 mm, 5 μm, Phenomenex). The mass spectrometer was operated in multiple reaction monitoring mode, and the quadrupole mass spectrometer equipped with an ESI source was optimized with the detection parameters as drying gas (N_2) flow 12 L/min, drying gas temperature 350 °C, nebulizer pressure 60 psig, capillary voltage 3.5 kV and capillary potential 4000 V. All the methods were validated for selectivity, linearity, precision, accuracy, extraction recovery, matrix effect and stability, according to the US Food and Drug Administration (FDA) guidance for validation of bioanalytical methods.

For the analysis of APAP-Cys in liver sample, isocratic elution was employed with mobile phase of methanol-10 mM ammonium acetate buffer solution containing 0.1% acetic acid (20:80, v/v) at a flow rate of 0.3 mL/min, the column temperature was maintained at 35 °C, and 5 μL were injected for analysis. The optimized MS/MS ion transition monitored were *m/z* 270.9/139.9 for APAP–CYS and *m/z* 285.1/193.1 for IS1 with the fragment voltage and collision energy were 80 V and 25 eV in positive ion mode.

For the analysis of 6-hydroxy-chlorzoxazone to evaluate the enzymatic activity of CYP2E1, isocratic elution was employed with mobile phase of methanol-5 mM ammonium acetate buffer solution containing 0.05% acetic acid (48:52, v/v) at a flow rate of 0.4 mL/min, the column temperature was maintained at 38 °C, and 3 μL were injected for analysis. The optimized MS/MS ion transition monitored were *m/z* 184.1/120.1 for 6-hydroxy-chlorzoxazone and *m/z* 150.0/107.0 for IS2 with the fragment voltage and collision energy were 95 V and 15 eV in negative ion mode.

For the analysis of 6β-hydroxy-testosterone and APAP to investigate the enzymatic activities of CYP3A4 and CYP1A2, gradient elution was employed with mobile phase of methanol-10 mM ammonium acetate buffer solution containing 0.1% formic acid at a flow rate of 0.35 mL/min. Gradient elution was as follows: 72% B (0–0.6 min), 72–46% B (0.6–0.8 min), 46% B (0.8–6.5 min), 46–35% B (6.5–6.7 min), 35% B (6.7–8.5 min), 35–72% B (8.5–8.7 min) and 72% B (8.7–13.5 min). The column temperature was maintained at 35 °C, and 8 μL were injected for analysis. The optimized MS/MS ion transition monitored were 305.3/269.3 for 6β-Hydroxy-testosterone, *m/z* 152.1/110.1 for APAP and *m/z* 385.3/91.0 for IS3 with the fragment voltage and collision energy were 110 V and 15 eV in positive ion mode.

2.9. Data analysis

Statistical analysis was performed using SPSS 16 software. Data was plotted in the figures as mean ± standard deviation (S.D.). Differences between two groups were assessed using two-tailed, unpaired Student's *t*-test with Welch's correction. Results were considered significant at $p < 0.05$.

3. Results

3.1. HO protected against APAP-induced liver damage

To investigate the effects of HO on the development of APAP-induced liver damage, mice were co-administrated with HO and APAP. The aminotransferase activities in serum are listed in Fig. 2A and B. The markers of hepatic damage components, ALT and AST, were elevated dramatically in APAP treated mice, but were markedly reduced during the co-treatment with HO. Similarly, APAP exposure resulted in decrement of GSH in liver, and this tendency was reversed by HO (Fig. 2C). Besides, H&E staining examination (Fig. 3) was performed on the liver for any abnormalities on the structure of the hepatocytes. The livers samples obtained from Vehicle group showed normal architecture and normal hepatic cells without fatty vacuolation. APAP challenge led to destruction of the normal hepatic architecture, necrosis of hepatocytes, hemorrhage and inflammatory cells infiltration, however, this pathological lesion was ameliorated when HO was co-treated. All of observations clearly illustrated that HO could protect against APAP-induced liver damage.

3.2. Influence of HO on the content of APAP-protein adducts in liver

Fig. 4A showed the chromatographic profiles of blank and APAP-treated liver homogenates. No interfering endogenous peaks were observed around their retention times. Liver samples were obtained 1 h after i.p. administration of APAP, as it has been described that APAP-protein adducts in liver are at a maximum at this point [13]. As shown in Fig. 5, the hepatic content of APAP-Cys was 0.63 ± 0.11 mmol/mg protein after administration of 400 mg/kg APAP, but that was decreased to 0.19 ± 0.05 mmol/mg protein after co-administrated with

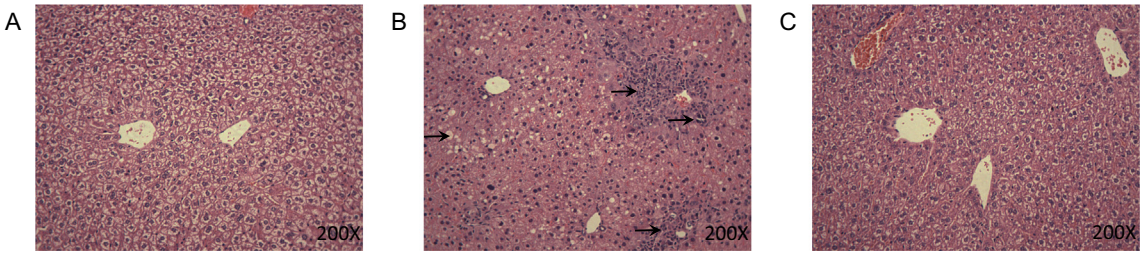

Fig. 3. Histomorphology of mouse liver (200× original magnification, H&E stained). Liver from (A) vehicle group, (B) APAP-treated group and (C) APAP and HO co-treated group.

100 mg/kg HO, which suggested that decreasing the generation of APAP-protein adducts might contribute the protective effect of HO on APAP-induced liver damage.

3.3. Influence of HO on activity of CYP450 metabolic enzyme

Fig. 4B showed the chromatographic profiles of blank and chlorzoxazone added incubation samples, and Fig. 4C exhibited the chromatographic profiles of blank as well as APAP and 6β-hydroxy-testosterone added incubation samples. No interfering endogenous peaks were observed around their retention times. The effects of HO and positive controls on CYP activities were determined from 8-point concentration data using cocktail substrates and the results were shown in Table 1. The positive controls strongly inhibited the CYPs, which indicated that the newly prepared mouse liver microsomes showed superior activity. HO potently and moderately inhibited the metabolic activities of CYP1A2 and CYP3A4 with the IC_{50} values of 3.95 ± 1.64 and 17.5 ± 6.7 μM, but not inhibited CYP3A4 with the IC_{50} value > 100 μM.

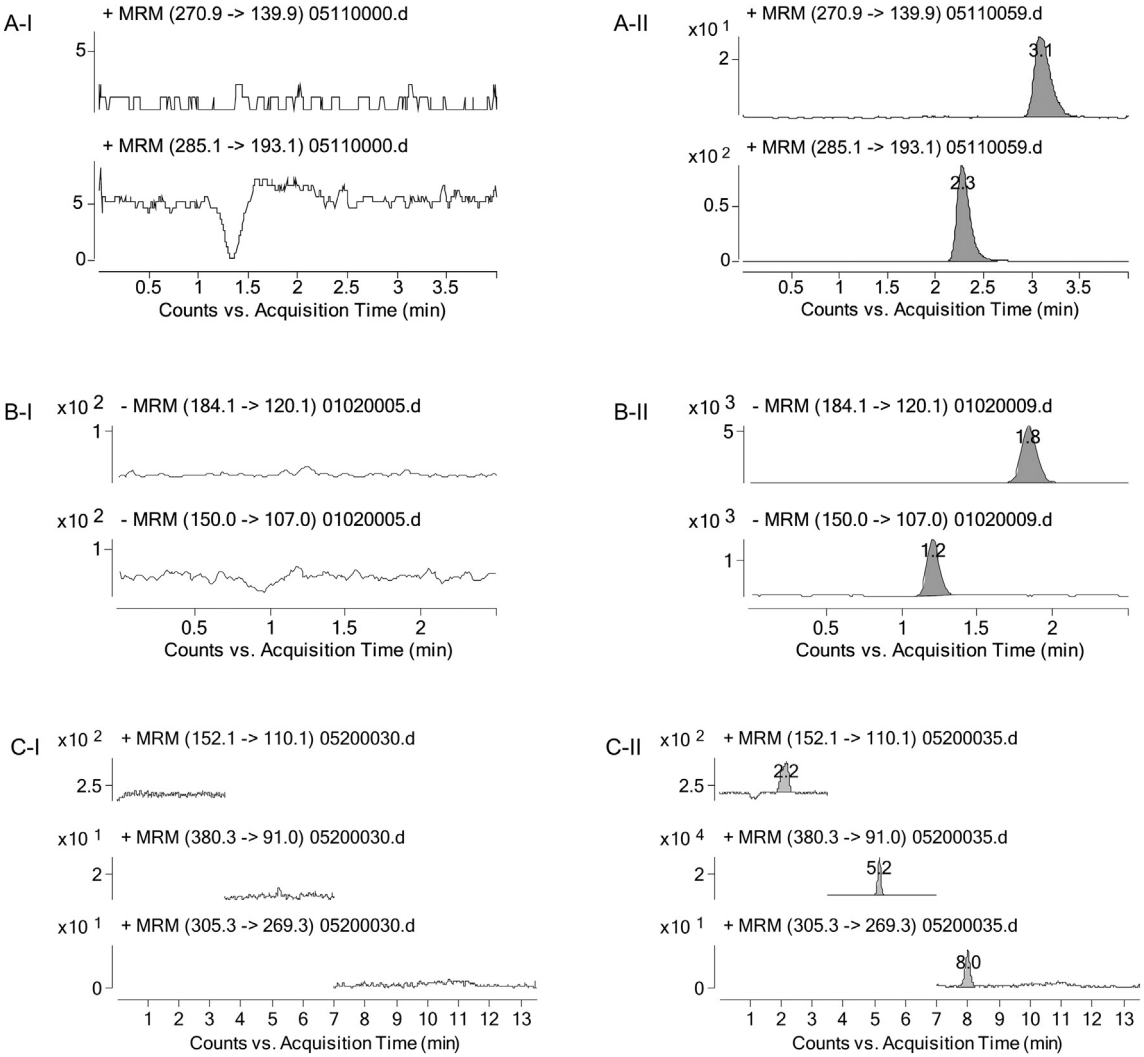

Fig. 4. Representative MRM chromatograms
(A) APAP-Cys, (B) 6-hydroxy-chlorzoxazone and (C) APAP and 6β-hydroxy-testosterone; I for blank samples and II for analyte containing samples.

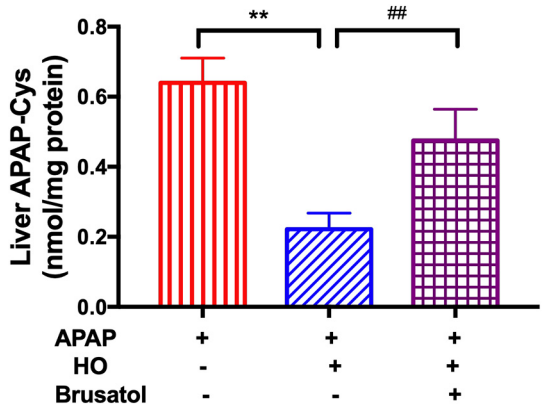

Fig. 5. Effects of HO on the content of APAP-Cys in liver. Data are represented as the mean ± S.D. of six independent experiments. $^{**}p < 0.01$ *vs.* vehicle group, and $\#\#p < 0.01$ *vs.* APAP-treated group.

Table 1
Effects of HO on CYP metabolic activity in pooled mouse liver microsomes (mean ± S.D., $n = 6$).

CYP	IC_{50} (μM)	
	HO	Positive control
2E1	3.95 ± 1.64	1.56 ± 1.05
2A1	17.5 ± 6.7	3.77 ± 1.10
3A4	> 100	0.57 ± 0.01

3.4. Influence of HO on the protein expression associated with GSH disposition in APAP treated mice

The relative levels of key protein involved in GSH biosynthesis (GCLC, GCLM and GS) and transfer enzyme (GST) were further studied. As shown in Fig. 6, the expression levels of the target proteins were slightly changed without statistical differences in APAP group compared with blank group, however, GCLC, GCLM and GST were dramatically elevated with significant differences when HO was co-administrated. These results show that elevating the protein expressions of GCLC, GCLM and GST might contribute to increasing the hepatic content of GSH and decreasing the generation of APAP-protein adducts.

3.5. Influence of HO on the protein expression of NRF2 in APAP treated mice

The nuclear factor (erythroid-derived 2)-like 2 (NRF2) plays a key role in the transactivation of GCLC, GCLM and GST. To examine whether HO affects GSH biosynthesis and transfer *via* inducing NRF2 nuclear translocation, protein expression of NRF2 was measured. Fig. 6 shows that the expression level of NRF2 was not affected by APAP, which was markedly increased by the co-administration of HO. There data suggested that NRF2 activation by HO might be associated with the regulations of GCLC, GCLM and GST.

3.6. Role of NRF2 in HO mediated hepatoprotective effect in APAP treated mice

To investigate the role of NRF2 on the hepatoprotective effect of HO on APAP treated mice, Brusatol, a specific NRF2 inhibitor [23,24], was used to research. When NRF2 was inhibited, the decreased APAP-protein adducts in liver was elevated (shown in Fig. 5), and the up-regulated protein expression levels of GCLC, GCLM and GST were reversed (shown in Fig. 6). All the observations provided evidence that the NRF2 pathway must be involved in the hepatoprotective effect of HO on APAP treated mice.

4. Discussion

HO exhibits extensive hepatoprotective effects, although whether HO could alleviate APAP-induced liver damage is still unclear. Thus, the current study aimed to investigate whether HO exerts a beneficial effect in preventing APAP-induced hepatotoxicity and what mechanisms are involved. The present data clearly demonstrated that HO exhibits hepatoprotective effects against APAP-induced liver damage, as evidenced by morphological and histological assessment, as well as biochemical data such as AST and ALT.

Generation of APAP-protein adducts induced by NAPQI and subsequent deactivation of functional proteins are regarded as the leading cause of APAP-induced liver damage [25]. Thus, in this study, the hepatic level of APAP-protein adducts in APAP-treated mice was further determined. The results clearly demonstrated that co-treatment with HO could decrease the hepatic level of APAP-protein adducts, as evidenced by decreased the content of APAP-Cys. The generation of APAP-protein adducts is dependent on the content of NAPQI [26], the electrophilic intermediate metabolite of APAP. Two manners could reduce the content of NAPQI in APAP treated mice, which are (1) inhibiting the activities of liver microsomes, that is reducing the generation of NAPQI [27], and/or (2) increasing the generation of GSH [28], that is accelerating the elimination of NAPQI. In this study, the influences of co-administration on those two manners were further investigated.

CYP2E1, CYP2A1 and CYP3A4 play important roles in the metabolism of APAP to NAPQI. Thus, the effect of HO on the activity of CYP2E1, CYP2A1 and CYP3A4 in APAP-treated mice was measured. Results from the *in vitro* substrate “cocktail” approach suggested that HO exhibits inhibitory effects on CYP2E1 and CYP2A1, but not CYP3A4, enzyme activities in APAP-treated mice, which was similar to that in type 2 diabetic rats [29]. The hepatic reduced GSH was also evaluated was evaluated and the results showed that the HO reversed APAP-induced reduction of GSH in APAP-treated mice. All of these data indicated that both decreasing the generation and accelerating the elimination of NAPQI contributed to the reduction of hepatic APAP-protein adducts in APAP treated mice.

The molecular mechanism related to the synthesis and transport of GSH was further researched. GSH is synthesized by amino acids *via* two ATP-requiring enzymatic steps in the cytosol of cells. The first step is considered to be the rate-limiting step and catalyzed by GCL, which is composed by GCLC, the catalytic subunit, and GCLM, the modifier subunit, whereas, the second step is catalyzed by GS [30,31]. Besides, the transport of GSH is regulated by GST, one of the most important phase II metabolic enzymes. In our experiment, APAP did not affect the protein expression levels of GCLC, GCLM, GS and GST, whereas when HO was co-administrated, the expressions of GCLC, GCLM and GST were up-regulated dramatically with the elevation of GSH. Therefore, it is confirmed that elevating the content of GSH and accelerating the elimination of NAPQI in APAP and HO co-treated mice were associated with altered the expression of GCLC, GCLM and GST.

The protein expression levels of GCLC, GCLM and GST are regulated by the gene of NRF2 [32]. Thus, the protein expression of NRF2 was further investigated. In the present study, HO treatment led to a significant increment in the protein expression of NRF2, indicating that NRF2 might be a key target in the protective effect of HO on APAP-induced liver damage. Further study discovered that NRF2 inhibition reduced the protein levels of GCLC, GCLM and GST, the concentration of GSH and APAP-protein adducts, and finally resulted in the depression of hepatoprotective effect of HO in APAP treated mice. All the observations verified that HO accelerates the generation of GSH in APAP-treated mice *via* activating the target of NRF2.

5. Conclusions

In summary, this study clearly demonstrated that HO could decrease the generation of APAP-protein adducts and protect against APAP-

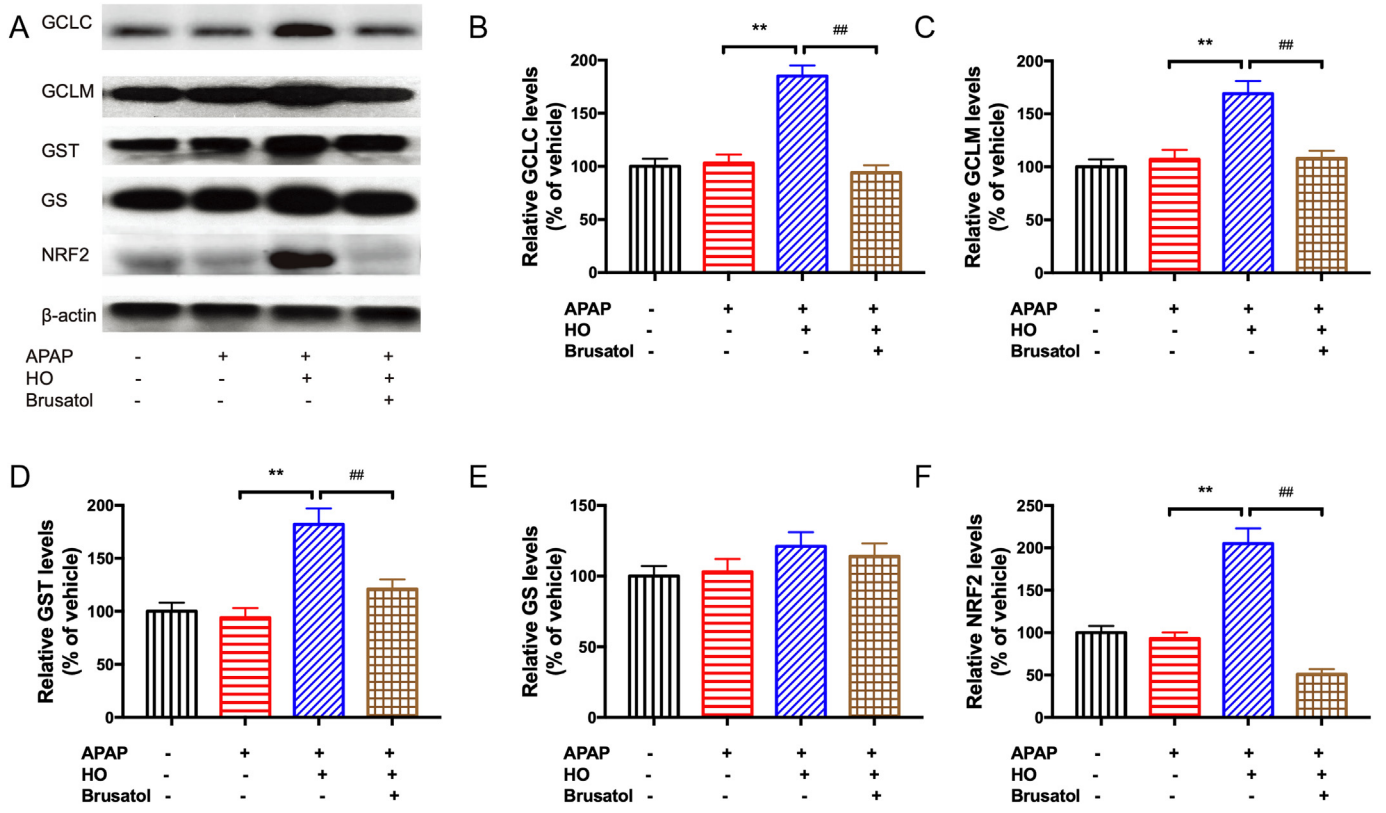

Fig. 6. Protein expressions related to the disposition of GSH. (A) western blot analysis of proteins associated with the disposition of GSH, and the bar graphs show quantitative relative level of (B) GCLC, (C) GCLM, (D) GS, (E) GST and (F) NRF2 protein expressions. Data are represented as the mean ± S.D. of six independent experiments. $^{**}p < 0.01$ *vs.* vehicle group, and $\#\#p < 0.01$ *vs.* APAP-treated group.

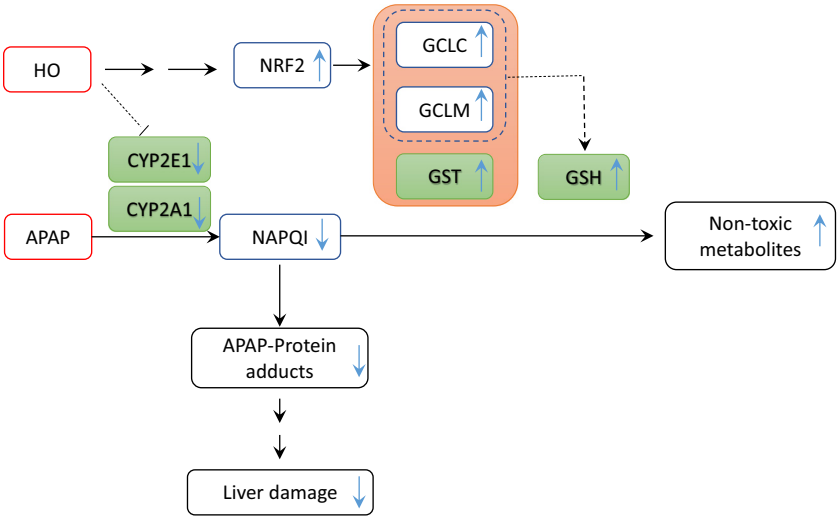

Fig. 7. Schematic diagram illustrating the potential protective mechanism of HO against APAP-induced liver damage. HO inhibits the activity of CYP2E1 and CYP2A1 and triggers the generation of GSH *via* activating the expression NRF2, reduces the generation of APAP-protein adducts, and finally alleviates APAP-induced hepatotoxicity.

induced liver injury, potentially through inhibiting the metabolic activities of CYP2E1 and CYP2A1, as well as elevating the expression of GCLC, GCLM and GST and accelerating the generation of GSH *via* NRF2 pathway (shown in Fig. 7).

Supplementary data to this article can be found online at https://doi.org/10.1016/j.lfs.2019.05.062.

Funding

This study was financially supported by the National Natural Science Foundation of China (No. 81873094 and No. 81503365) and the Natural Science Foundation of Jiangsu Province, China (No. BK20151050).

Declaration of Competing Interest

The authors report no conflict of interests.

References

[1] K.R. Olson, A.H. Davarpanah, E.A. Schaefer, N. Elias, J. Misdraji, Case 2-2017. An 18-year-old woman with acute liver failure, N. Engl. J. Med. 376 (2017) 268–278, https://doi.org/10.1056/NEJMcpc1613467.

[2] E.J. Nam, K. Hayashida, R.S. Aquino, J.R. Couchman, R.A. Kozar, J. Liu, P.W. Park, Syndecan-1 limits the progression of liver injury and promotes liver repair in

acetaminophen-induced liver injury in mice, Hepatology 66 (2017) 1601–1615, https://doi.org/10.1002/hep.29265.
[3] S. Xu, J. Liu, J. Shi, Z. Wang, L. Ji, 2,3,4′,5-Tetrahydroxystilbene-2-O-beta-D-glucoside exacerbates acetaminophen-induced hepatotoxicity by inducing hepatic expression of CYP2E1, CYP3A4 and CYP1A2, Sci. Rep. 7 (2017) 16511, , https://doi.org/10.1038/s41598-017-16688-5.
[4] Y. Ohtsuki, S. Sanoh, M. Santoh, Y. Ejiri, S. Ohta, Y. Kotake, Inhibition of cytochrome P450 3A protein degradation and subsequent increase in enzymatic activity through p38 MAPK activation by acetaminophen and salicylate derivatives, Biochem. Biophys. Res. Commun. 509 (2019) 287–293, https://doi.org/10.1016/j.bbrc.2018.12.124.
[5] N.U. Nguyen, B.D. Stamper, Polyphenols reported to shift APAP-induced changes in MAPK signaling and toxicity outcomes, Chem. Biol. Interact. 277 (2017) 129–136, https://doi.org/10.1016/j.cbi.2017.09.007.
[6] D. Chen, H.M. Ni, L. Wang, X. Ma, J. Yu, W.X. Ding, L. Zhang, p53 up-regulated modulator of apoptosis induction mediates acetaminophen-induced necrosis and liver injury in mice, Hepatology 69 (2019) 2164–2179, https://doi.org/10.1002/hep.30422.
[7] V. Behrends, G.F. Giskeodegard, N. Bravo-Santano, M. Letek, H.C. Keun, Acetaminophen cytotoxicity in HepG2 cells is associated with a decoupling of glycolysis from the TCA cycle, loss of NADPH production, and suppression of anabolism, Arch. Toxicol. 93 (2019) 341–353, https://doi.org/10.1007/s00204-018-2371-0.
[8] H.M. Ni, M.R. McGill, X. Chao, K. Du, J.A. Williams, Y. Xie, H. Jaeschke, W.X. Ding, Removal of acetaminophen protein adducts by autophagy protects against acetaminophen-induced liver injury in mice, J. Hepatol. 65 (2016) 354–362, https://doi.org/10.1016/j.jhep.2016.04.025.
[9] N. Guldiken, Q. Zhou, O. Kucukoglu, M. Rehm, K. Levada, A. Gross, R. Kwan, L.P. James, C. Trautwein, M.B. Omary, P. Strnad, Human keratin 8 variants promote mouse acetaminophen hepatotoxicity coupled with c-jun amino-terminal kinase activation and protein adduct formation, Hepatology 62 (2015) 876–886, https://doi.org/10.1002/hep.27891.
[10] S.F. Cook, A.D. King, Y. Chang, G.J. Murray, H.R. Norris, R.C. Dart, J.L. Green, S.C. Curry, D.E. Rollins, D.G. Wilkins, Quantification of a biomarker of acetaminophen protein adducts in human serum by high-performance liquid chromatography-electrospray ionization-tandem mass spectrometry: clinical and animal model applications, J. Chromatogr. B Analyt. Technol. Biomed. Life Sci. 985 (2015) 131–141, https://doi.org/10.1016/j.jchromb.2015.01.028.
[11] M. Acharya, C.A. Lau-Cam, Simple reversed-phase HPLC method with spectrophotometric detection for measuring acetaminophen-protein adducts in rat liver samples, The Scientific World J 2012 (2012) 145651, , https://doi.org/10.1100/2012/145651.
[12] M.R. McGill, M. Lebofsky, H.R. Norris, M.H. Slawson, M.L. Bajt, Y. Xie, C.D. Williams, D.G. Wilkins, D.E. Rollins, H. Jaeschke, Plasma and liver acetaminophen-protein adduct levels in mice after acetaminophen treatment: dose-response, mechanisms, and clinical implications, Toxicol. Appl. Pharmacol. 269 (2013) 240–249, https://doi.org/10.1016/j.taap.2013.03.026.
[13] K.L. Muldrew, L.P. James, L. Coop, S.S. McCullough, H.P. Hendrickson, J.A. Hinson, P.R. Mayeux, Determination of acetaminophen-protein adducts in mouse liver and serum and human serum after hepatotoxic doses of acetaminophen using high-performance liquid chromatography with electrochemical detection, Drug Metab. Dispos. 30 (2002) 446–451, https://doi.org/10.1124/dmd.30.4.446.
[14] M.S. Seo, J.H. Kim, H.J. Kim, K.C. Chang, S.W. Park, Honokiol activates the LKB1-AMPK signaling pathway and attenuates the lipid accumulation in hepatocytes, Toxicol. Appl. Pharmacol. 284 (2015) 113–124, https://doi.org/10.1016/j.taap.2015.02.020.
[15] V.B. Pillai, S. Samant, N.R. Sundaresan, H. Raghuraman, G. Kim, M.Y. Bonner, J.L. Arbiser, D.I. Walker, D.P. Jones, D. Gius, M.P. Gupta, Honokiol blocks and reverses cardiac hypertrophy in mice by activating mitochondrial Sirt3, Nat. Commun. 6 (2015) 6656, , https://doi.org/10.1038/ncomms7656.
[16] K. Sulakhiya, P. Kumar, S.S. Gurjar, C.C. Barua, N.K. Hazarika, Beneficial effect of honokiol on lipopolysaccharide induced anxiety-like behavior and liver damage in mice, Pharmacol. Biochem. Behav. 132 (2015) 79–87, https://doi.org/10.1016/j.pbb.2015.02.015.
[17] X. Zhong, H. Liu, Honokiol attenuates diet-induced non-alcoholic steatohepatitis by regulating macrophage polarization through activating peroxisome proliferator-activated receptor γ, J. Gastroenterol. Hepatol. 33 (2018) 524–532, https://doi.org/10.1111/jgh.13853.
[18] Y.H. Jeong, H.J. Hur, E.J. Jeon, S.J. Park, J.T. Hwang, A.S. Lee, K.W. Lee, M.J. Sung, Honokiol improves liver steatosis in ovariectomized mice, Molecules 23 (2018) 194, https://doi.org/10.3390/molecules23010194.
[19] J.X. Liu, S.N. Shen, Q. Tong, Y.T. Wang, L.G. Lin, Honokiol protects hepatocytes from oxidative injury through mitochondrial T deacetylase SIRT3, Eur. J. Pharmacol. 834 (2018) 176–187, https://doi.org/10.1016/j.ejphar.2018.07.036.
[20] T. Hairin, A.R. Marzilawati, E.M.H. Didi, S. Mahadeva, Y.K. Lee, N.A. Rahman, A.M. Mustafa, Z. Chik, Quantitative LC/MS/MS analysis of acetaminophen–cysteine adducts (APAP–CYS) and its application in acetaminophen overdose patients, Anal. Methods 5 (2013) 1955–1964, https://doi.org/10.1039/C3AY26614A.
[21] S.T. Stern, M.K. Bruno, G.E. Hennig, R.A. Horton, J.C. Roberts, S.D. Cohen, Contribution of acetaminophen-cysteine to acetaminophen nephrotoxicity in CD-1 mice: I. enhancement of acetaminophen nephrotoxicity by acetaminophen-cysteine, Toxicol. Appl. Pharmacol. 202 (2005) 151–159, https://doi.org/10.1016/j.taap.2004.06.030.
[22] F.L. Yu, W.L. Gong, F.J. Xu, J.W. Wu, S. Shakya, H. Zhu, Influence of nutritional status on the absorption of polyphyllin I, an anticancer candidate from Paris polyphylla in rats, Eur. J. Drug Metab. Pharmacokinet. 43 (2018) 587–597, https://doi.org/10.1007/s13318-018-0473-y.
[23] D. Ren, N.F. Villeneuve, T. Jiang, T. Wu, A. Lau, H.A. Toppin, D.D. Zhang, Brusatol enhances the efficacy of chemotherapy by inhibiting the Nrf2-mediated defense mechanism, Proc. Natl. Acad. Sci. U. S. A. 108 (2011) 1433–1438, https://doi.org/10.1073/pnas.1014275108.
[24] S. Tao, S. Wang, S.J. Moghaddam, A. Ooi, E. Chapman, P.K. Wong, D.D. Zhang, Oncogenic KRAS confers chemoresistance by upregulating NRF2, Cancer Res. 74 (2014) 7430–7441, https://doi.org/10.1158/0008-5472.CAN-14-1439.
[25] E.M. Lancaster, J.R. Hiatt, A. Zarrinpar, Acetaminophen hepatotoxicity: an updated review, Arch. Toxicol. 89 (2015) 193–199, https://doi.org/10.1007/s00204-014-1432-2.
[26] S.R. McGreal, B. Bhushan, C. Walesky, M.R. McGill, M. Lebofsky, S.E. Kandel, R.D. Winefield, H. Jaeschke, N.E. Zachara, Z. Zhang, E.P. Tan, C. Slawson, U. Apte, Modulation of O-GlcNAc levels in the liver impacts acetaminophen-induced liver injury by affecting protein adduct formation and glutathione synthesis, Toxicol. Sci. 162 (2018) 599–610, https://doi.org/10.1093/toxsci/kfy002.
[27] Y. Jiang, X. Fan, Y. Wang, P. Chen, H. Zeng, H. Tan, F.J. Gonzalez, M. Huang, H. Bi, Schisandrol B protects against acetaminophen-induced hepatotoxicity by inhibition of CYP-mediated bioactivation and regulation of liver regeneration, Toxicol. Sci. 143 (2015) 107–115, https://doi.org/10.1093/toxsci/kfu216.
[28] S.I. Gum, M.K. Cho, The amelioration of N-acetyl-p-benzoquinone imine toxicity by ginsenoside Rg3: the role of Nrf2-mediated detoxification and Mrp1/Mrp3 transports, Oxidative Med. Cell. Longev. 2013 (2013) 957947, , https://doi.org/10.1155/2013/957947.
[29] J. Wang, T. Zhai, Y. Chen, Effects of Honokiol on CYP450 activity and transporter mRNA expression in type 2 diabetic rats, Int. J. Mol. Sci. 19 (2018) 815, https://doi.org/10.3390/ijms19030815.
[30] H. Zhu, M.H. Long, J. Wu, M.M. Wang, X.Y. Li, H. Shen, J.D. Xu, L. Zhou, Z.J. Fang, Y. Luo, S.L. Li, Ginseng alleviates cyclophosphamide-induced hepatotoxicity via reversing disordered homeostasis of glutathione and bile acid, Sci. Rep. 5 (2015) 17536, , https://doi.org/10.1038/srep17536.
[31] S.C. Lu, Regulation of glutathione synthesis, Mol. Asp. Med. 30 (2009) 42–59, https://doi.org/10.1016/j.mam.2008.05.005.
[32] S.C. Lu, Glutathione synthesis, Biochim. Biophys. Acta 1830 (2013) 3143–3153, https://doi.org/10.1016/j.bbagen.2012.09.008.